Feasibility of Wheel-Based Magnetostrictive Energy Harvester

Y. W. Park[*,**] and N. M. Wereley[**]

[*]Chungnam National University, Department of Mechatronics Engineering
99 Daehak-ro, Yuseong-gu, Daejeon 305-764, Republic of Korea, ywpark@cnu.ac.kr
[**]University of Maryland, College Park, MD, USA, wereley@umd.edu

ABSTRACT

This paper presents the feasibility of a wheel-based magnetostrictive energy harvester (MEH), which consists of one coil-wound Galfenol cantilever with two PMs adhered onto the each end, and one PM array sandwitched between two wheels. Simulation is used to validate the concept. The proof-of-concpet MEH is fabricated by using the simulation results, and subjected to the experimental characterization. Two experimental setups are used to study the feasibility of wheel-based MEH: one with magnetostrictive acuator, and the other with the motor-driven PM array. It can be concluded that Generated voltage peaks near resonance of the cantilever and increases with rpm and with number of coil-turns. Future work includes optimization of wheel-based MEH performance via PM array configuration, and development of protptype.

Keywords: magnetostrictive energy harvester, frequency rectification, Galfenol, permannent magnet, pole configuration

1 INTRODUCTION

Shopping carts are easily found around us due to their provision of shopping easiness. Although this fact makes shopping enjoyable, one serious problem arises, the bottleneck at checkout. A self checkout is one of current solutions, but still not common. One reason seems that it is not user-friendly. Thus, a smarter way is really needed.

One possible appraoch is to use a wireless sensor network, which consists of a bar code or RFID, a reader, network, and power supply. If an active RFID-attached product is placed in a cart, a RFID reader on the cart can retrieve price and related information on the RFID, and store it for further processing. In this system, power supply is the most critical. Currently possible power supply may be a rechargeable or disposable battery for the reader. The proposed idea is to harvest electricity from the manually-pushed rotating wheels, and to operate the reader with the harvested electricity. Thus, this paper presents the feasibility of a wheel-based magnetostrictive energy harvester (MEH). The proposed MEH converts vibration from the manually-pushed cart to electricity by using the magnetostrictive effect and non-contact frequency rectifcatification. Non-contact frequency rectification is not new [1], but the use of a rotary PM array is a new concept.

2 DESIGN AND SIMULATION

2.1 Concept

Galfenol is an iron-galium alloy invented by US Navy, and is a magnetostrictive material. The most notable feature of this material compared to another magnetostrictive material, Terfenol-D, is ductility, which makes it operable in bending mode. The concept for the wheel-based MEH is utilizing this feature of Galfenol with rotating magnetic field for frequency rectification. MEH is composed of one coil-wound Galfenol cantilever with two PMs adhered onto the each end, and one PM array sandwitched between two wheels. The operating principle is as follows: As the PM array rotates, the cantilever is subjected to repeatitive repulsive and attractive magnetic forces generated from the PM array, hence causing the cantilever bent. As the cantilever gets bent, a compressive stress is applied to one side, and a tensile one to the other side along the longitudinal direction. The inverse magnetostrictive effect causes a change of the flux due to the applied stress, resulting in generation of electricity. This relationship is Farady's law of induction and expressed as

$$V = N\frac{d\Phi}{dt} = d_G A_G N\frac{dT}{dt} \quad (1)$$

, where, V is a generated electricity in volts, N the number of coil-turns, $d\phi/dt$ the time-rate of change of magnetic flux, d_G a magnetic constnat, A_G the cross-sectional area of the cantilever, and dT/dt the time-rate of change of stress.

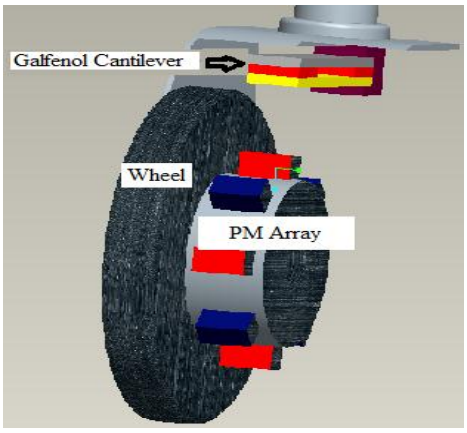

Figure 1: Concept.

2.2 Simulation

Before going into immediate simulation, some estimation is needed for safer operation of EH as well as for simulation. The first thing to know is a maximum allowable load at the free end of the cantilever. The maximum load is calculated to be 13 N considering maximum tensile strength of Galfenol is 350 MPa and safety factor 6. The distance between two PMs (one on the cantilever, and the other on the PM array), *G*, is the next to be determined. The closed form solution is used for evaluating the distance [2], and is expressed as

$$G = \frac{B_r A}{2\sqrt{\pi \mu_0 F}} - t \qquad (2)$$

, where, B_r is the magnetic flux density, A the cross-sectional area of the PM, μ_0 the permeability of free space, F the magnetic force, and t the thickness of the PM.

It is evaluated to be 8 mm considering the maximum load and physical properties of NdFeB37.

Simulation using a shareware in public domain, FEMM 4.2, is conducted to design a proper PM configuration on the cantilever and on the PM array. The objective of simulation is to maximize the magnetic flux along the cantilever in the lengthwise direction according to configuration of the PMs. Two types of configuration are of concern in this study: one for two PMs apart on the cantilever, and the other for the PM on the free end of the cantilever and the PMs on the PM array.

The conditions for simulation are as follows: The dimension (*L* x *W* x *T*) of the Galfenol cantilever and of PM are 100 x 15 x 3 mm^3 and 15 x 10 x5 mm^3, respectively. G is set to 8 mm, as estimated before. PMs used are NdFeB37, and permeability of Galfenol is given to . Only three PMs on the PM array are modelled for simplicity, although total numbers of the PM are twelve.

The first simulation is to test the effect of the pole directions of the PMs apart on the cantilever. Figure 2 shows PM configuration and corresponding flux lines on the cantilever, and the flux density (B(T)) and flux intensity (H(A/m)) along it.

In Figure 2(a), most of the flux lines in the antiparallel pole configuration are attracted to each other, compared to the flux lines in the parallel pole configuration. Also, the antiparallel configuration induces higher flux density than parallel one, although the flux intensities in both configurations are not discernable. Therefore, the antiparallel configuration is selected for further simulation.

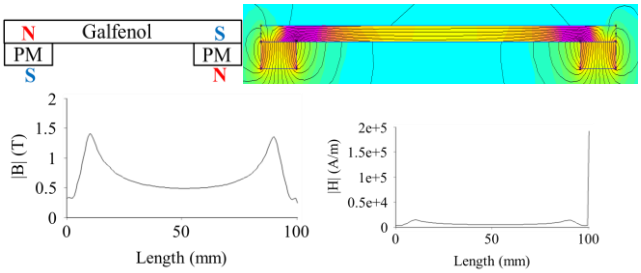

(a) Antiparallel pole.

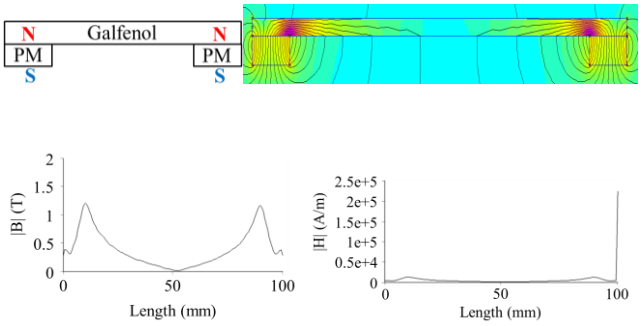

(b) Parallel pole.

Figure 2: Effect of pole configuration on cantilever.

The second simulation is to test the effect of pole directions between the PM on the free end of the cantilever (canPM) and the corresponding PM on the PM array (corPM), and between the PMs on the PM array (neighborPMs).

Figure 3(a) shows the parallel pole of the canPM and the corPM, and antiparallel pole of the neighborPMs. Most flux lines from the corPM are attracted to the can PM, but some flux leakage is found from the neighbor PMs.

Figure 3(b) shows the parallel pole of canPM and the corPM, and also parallel pole of the neighborPMs. More flux lines from the corPM and neighborPMs are attracted to the canPM, which induces higher and more uniform flux density and flux intensity. It can be confirmed by checking the flux density and flux intensity along the cantilever. It is likely that the flux from neighborPMs flows toward the corPM and consequently toward the canPM.

Figure 3(c) shows the antiparallel pole of the canPM and the corPM, and also antiparallel pole of the neighborPMs. Most flux lines interact between the neighborPMs, and weaker interaction is found between the canPM and neighborPMs.

Figure 3(d) shows the antiparallel pole of the canPM and the corPM, and parallel pole of the neighborPMs. Most flux lines interact between the neighborPMs, and stronger interaction is found between the canPM and neighborPMs.

Therefor,the configuration with the parallel pole of canPM and the corPM, and with parallel pole of the neighborPMs is selected for fabrication.

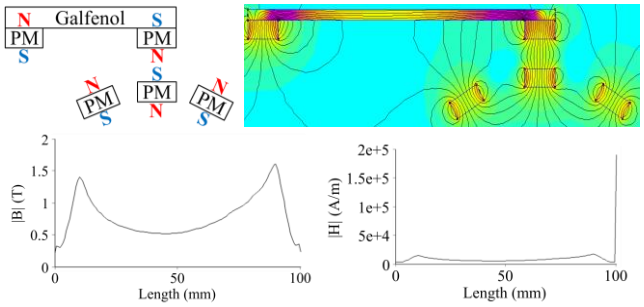

(a) Parallel pole of the canPM and the corPM, and antiparallel pole of the neighborPMs.

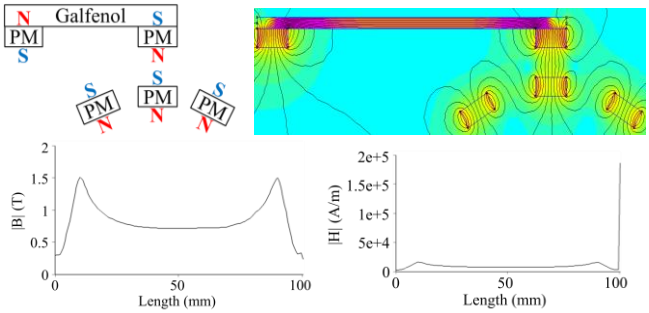

(b) Parallel pole of canPM and corPM, and the same pole of neighborPMs.

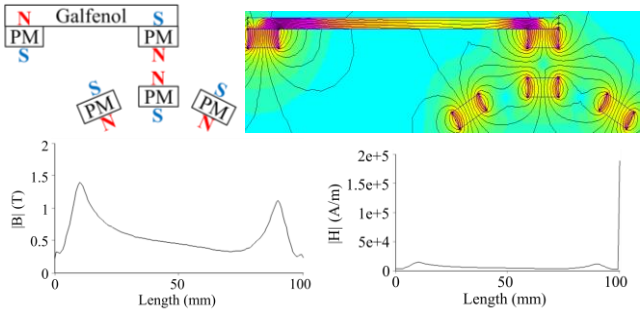

(c) Antiparallel pole of canPM and corPM, and the same pole of the neighborPMs.

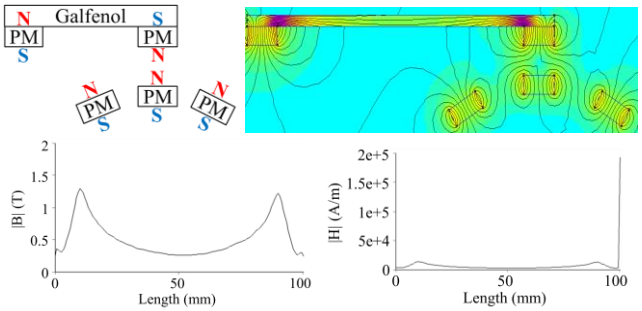

(d) Antiparallel pole of canPM and corPM, and parallel pole of neighborPMs.

Figure 3: Effect of pole configuration on PM array.

3 FABRICATION AND TESTING

3.1 Fabrication

The fabrication of MEH is based on simulation result. Figures 4 shows a proof-of-concept of PM array. Figure 4(a) shows 3-D modeled and fabricated PM array. Core is made of a plastic, and machined to make seats for the PMs. Figure 4(b) shows the partially assebled wheel and PM array. The coil-wound Galfenol cantilever is clamped on a gripper, and the PM array with two wheels is fixed by using aluminim profile.

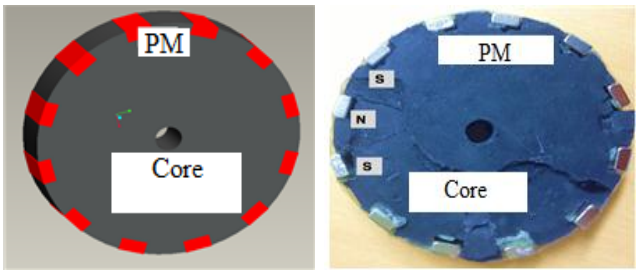

(a) Figure 2: Modeled and fabricated PM array.

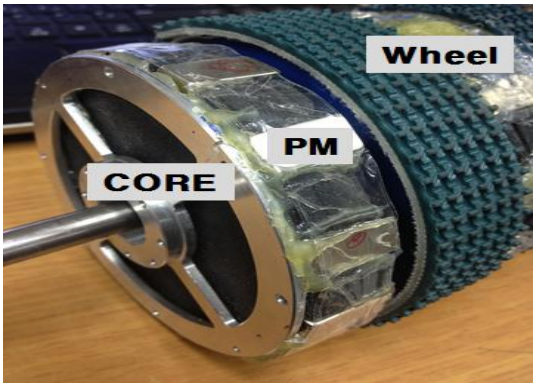

(b) Assembled wheel and PM array.

Figure 4: Proof-of concept.

3.2 Testing

Two experimental setups, as shown in Figure 5, are used to study the feasibility of wheel-based MEH: one with magnetostrictive acuator, and the other with the motor-driven PM array. In the figure, the input lines (a) and (b) are for the magnetostrictive actuator, and for the motor, respectively. The output line is to measure the generated voltage from the EH. The first setup for the fundamental characterization uses a magnetostrictive actuator to induce vibration on the free end of the cantiever. It aims to observe whether electricicty is generated by induced vibeation, and to know which frequency the maximum electricity is generated at. The second setup for the simulated

characterization uses the motor-driven PM array to induce a forced vibration.

The experimental configuration for the first experiment is EH without PM, with one PM, with two PMs, without path, with a path thickness of 0.3mm and of 3 mm. The displacement of the magnetostrictive is set to μm.

The experimental configuration for the second experiement is EH with different rpm of the motor (50 to 300), and with different number of coil-turns (100 to 1k).

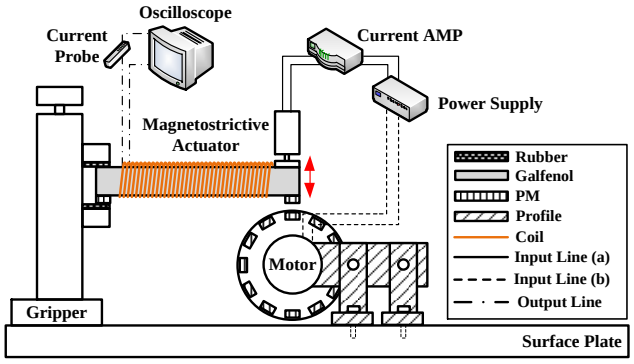

Figure 5: Experimental setup.

4 RESULTS AND DISCUSSION

Figure 6 shows the generated voltage versus applied frequency from the fundamental characterization. The generated voltage increases as frequency increases upto around 125 Hz, but decreases with further increase of frequency. It is likely that generated voltage peaks near resonance of the cantilever. The magnitude of the generated voltage is relatively small, compared to the data found in the literature [3]. It may be due to the small displacements of the magnetostrictive actuator. It would be expected to get higher voltages, if bigger displacements are applied.

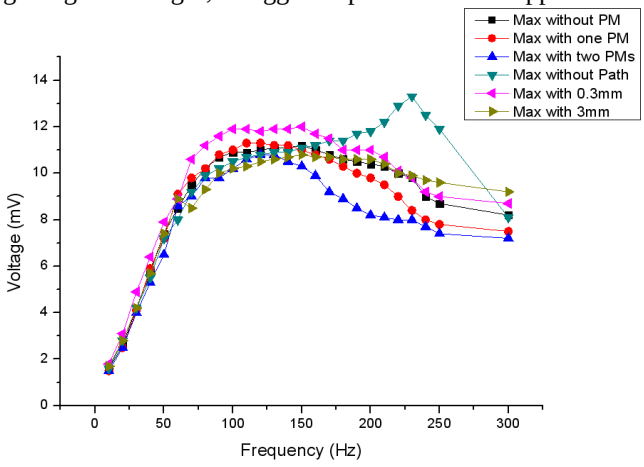

Figure 6: Generated voltage vs. frequency.

Figure 7 shows the generated voltage versus rpm from the motor-driven PM array. The generated voltage increases with the increase of rpm. The magnitude of the generated voltage is much higher than that with the fundamental characterization. It reaches about 900 mV at a rpm of 300, and is comparable to the data found in the literature [3]. The frequency at 300 rpm is estimated to be 60Hz. The slope of the curves increase as the number of coil-turns on the cantilever increases. The percent increase of the generated voltage from 50 rpm to 300 rpm is about 1160 percent with 1000 coil-turns, but is about 270 percent with 100 coil-turns.

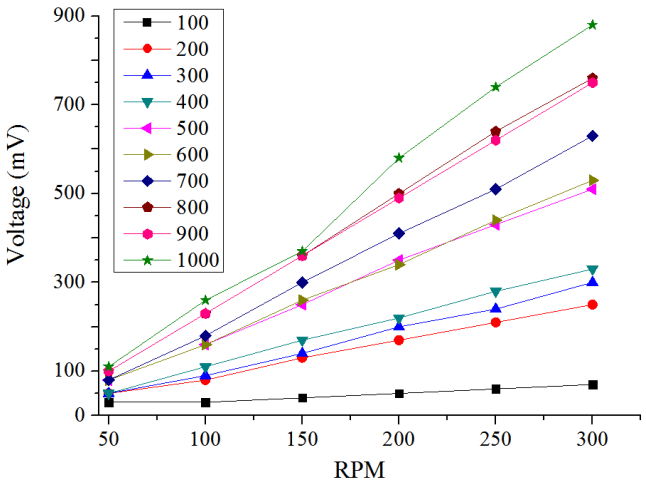

Figure 7: Generated voltage vs. RPM.

5 CONCLUSIONS AND FUTURE WORK

Wheel-based MEH is conceptualized, simulated, fabricated, and characterized. Conclusions can be drawn as follows:

1) Generated voltage peaks near resonance of the cantilever.
2) Wheel-based MEH spectrum can be widened via PM array design.
3) Generated voltage increases with RPM.
4) Wheel-based MEH is driven by using a motor.

Future work includes optimization of wheel-based MEH performance via PM array configuration, and development of protptype.

REFERENCES

[1] T. Chung, D. Lee, M. Ujihara and G. Carmen, "Design, Simulation, and Fabrication of a Novel Vibration-based Magnetic Energy Harvesting Device," Proceedings of Transducers & Eurosensors '07, 2007.

[2] G. Akoun and J. P. Yonnet, "3D Analytical Calculation of the Forces Exerted between Two Cubiodal Magnets," IEEE Transactions on Magnetics, Vol. 20, No. 5, pp.1962-1964 , 1984.

[3] T. Ueno and S. Yamada, "Performance of Energy Harvester Using Iron–Gallium Alloy in Free Vibration," IEEE Transactions on Magnetics, Vol. 47, No. 10, pp.2407-2409 , 2011.